A new group of low-spin $50-70M_{\odot}$ Black Holes and the high pair-instability mass cutoff

Yuan-Zhu Wang (王远瞩),^{1,*} Yin-Jie Li (李银杰),^{2,*} Shi-Jie Gao (高世杰),^{3,4} Shao-Peng Tang (唐少鹏),² and Yi-Zhong Fan (范一中)^{2,5,†}

¹Institute for Theoretical Physics and Cosmology, Zhejiang University of Technology, Hangzhou, 310032, People's Republic of China

²Key Laboratory of Dark Matter and Space Astronomy, Purple Mountain Observatory,

Chinese Academy of Sciences, Nanjing 210023, People's Republic of China

³School of Astronomy and Space Science, Nanjing University, Nanjing, 210023, People's Republic of China

⁴Key Laboratory of Modern Astronomy and Astrophysics, Nanjing University,

Ministry of Education, Nanjing, 210023, People's Republic of China

⁵School of Astronomy and Space Science, University of Science and

Technology of China, Hefei, Anhui 230026, People's Republic of China

Pair-instability supernovae (PISN) will not leave compact remnants and hence yield a mass gap of the black holes. Though a transition point of $\sim 45 M_{\odot}$ between low-spin and high-spin black holes groups had been inferred with gravitational wave data since 2022 and then interpreted as the signature of the PISN mass gap, here we report the emergence of a *new* group of low-spin but massive ($\sim 50-70 M_{\odot}$) black holes, which are hard to produce via hierarchical mergers, in the latest GWTC-4.0 data. Correspondingly, the mass cutoff of the low-spin black holes shifts to $68.5^{+19.8}_{-18.5} M_{\odot}$ (90% credibility), which is consistent with the PISN model for a low $^{12}C(\alpha,\gamma)^{16}O$ reaction rate of $S_{300 \rm keV} \sim 110~\rm keV$ b. Despite that the massive single-star collapse/dynamical capture origin can not be reliably tested at this moment, a high pair-instability mass cutoff $M_{\rm low} \sim 70 M_{\odot}$ may be favored for its capability of accounting for the rather low observation rate of hydrogen-less super-luminous supernovae.

Introduction. The direct detection of gravitational waves (GWs) from binary black hole (BBH) mergers by Advanced LIGO and Virgo has inaugurated a new era of observational astrophysics [1]. This breakthrough has provided an unprecedented tool for testing general relativity in the strong-field regime [2-4] and, crucially, for studying the population of stellar-mass BHs, which are otherwise hardly visible to electromagnetic observatories [5, 6]. One of the key goals of the population studies of the BBH events is to find the evidence for the (pulsational) pairinstability supernovae (PISN [7]) that are predicted to leave no BHs within the mass range of (M_{low}, M_{high}) , where $M_{
m low} \sim 50-65{
m M}_{\odot}$ and $M_{
m high} \sim 120-130{
m M}_{\odot}$ [8-11], commonly referred to as the pair-instability mass gap (PIMG). The existence, edges, and detailed structure of this gap are highly sensitive to the properties of massive stellar progenitors, such as their metallicity, rotation, and massloss rates [11, 12].

The first gravitational-wave transient catalog (GWTC-1) resulted in a preliminary hint for a cutoff in the primary mass distribution at $\sim 45 {\rm M}_{\odot}$ [13], which however has been challenged by the more massive black holes identified in subsequent observations. Considering the plausible presence of a high-mass BH component resulting from hierarchical mergers [5, 14, 15], Wang et al. [16] identified a cutoff feature at $m_{\rm c}\approx 50 M_{\odot}$ in the GWTC-2 data, and interpreted it as the $M_{\rm low}$, in view of its consistency with the stellar evolution models (see also [17]). Motivated by such a progress, in 2022 Wang et al. [18] further constructed phenomenological models containing two subpopulations, and found out that the black holes in GWTC-3 can indeed be well described by two components characterized by their different mass/spin features. In the dedicated

analysis focusing on spin magnitudes, it turns out that the spin amplitude of component BHs can be divided into two groups with a division mass $m_{\rm d}=46.1^{+5.6}_{-5.1}M_{\odot}$ [18], comparable to the cutoff mass $m_{\rm c}$ in [16], and has been taken as the signature of the PISN. This two subpopulation scenario, and in particular, the presence of a truncated mass of the low-mass/spin sub-population at $\approx 45 M_{\odot}$ have been further supported by Li et al. [19] using a flexible mixture model for the component-mass versus spin-magnitude distribution of GWTC-3 BHs. Owing to their robust analysis, those authors interpreted this as evidence for the pairinstability explosions of massive stars. Subsequent studies with the same dataset have obtained similar results using different approaches [20–24].

Very recently, the GWTC-4.0 data are available and the BBH event sample has increased significantly [25]. With these data, Tong et al. [26] found a cut-off mass of $45^{+5}_{-4}\mathrm{M}_{\odot}$ in the spectrum of secondary mass (see however Ref.[27] for different opinion with a more flexible mass function). Antonini et al. [28] reported a rapid transition at $45.3^{+6.5}_{-4.8} \rm{M}_{\odot}$ between two subpopulations with different $\chi_{\rm eff}$ distributions (in the primary-mass function), which is almost identical to $m_{\rm d}=46.1^{+5.6}_{-5.1}M_{\odot}$ found in the spin magnitude analysis by Wang et al. [18] with GWTC-3 data. Similar results are also presented in some other analysis based on GWTC-4.0 [29–31]. While these new/improved constraints are broadly consistent with earlier results mentioned above (and the cutoff at $\sim 45 M_{\odot}$ has been attributed to the PISN explosions), we *notice* that a group of low-spin yet massive ($\gtrsim 60 M_{\odot}$) black holes has emerged in the O4a data (see Figure 1). These black holes are unusual, as they are difficult to produce via hierarchical mergers, and may instead point to either a low ${}^{12}C(\alpha,\gamma){}^{16}O$

reaction rate [11] or formation from massive stars whose envelopes were not stripped [32].

Population models. Based on the mixture formula in Li et al. [19], the distribution in component mass and spin parameter space is

$$\pi(m, \chi, \cos \theta | \Lambda) = \sum_{i=1,2} r_i P_{m,i}(m | \Lambda_i) P_{\chi,i}(\chi | \Lambda_i) P_{\cos \theta,i}(\cos \theta | \Lambda_i),$$
 (1)

where i = 1, 2 denotes there could be two different subpopulations of component BHs, and r_i is the branch ratio of each subpopulation in the underlying distribution. Thanks to the significantly enriched data of GWTC-4, we adopt a comprehensive data-driven model, where all the component-mass, spin-magnitude and cosine-tilt-angle distributions $(P_{m,i}(m|\Lambda_i), P_{\chi,i}(\chi|\Lambda_i), P_{\cos\theta,i}(\chi|\Lambda_i))$ are described with cubic spline functions [33]. Especially for the mass function of first (second) subpopulation, we use 15 (10) knots linearly in log space between $[6, 100]M_{\odot}$ $([10,150]M_{\odot})$ to interpolate the perturbation. Such a configuration is more flexible than that of previous work [19, 34], where 12 knots are use between $[6, 80]M_{\odot}$. This is because in this work, we aim to determine the mass distributions of the two subpopulations in details, especially the edges. Please see Appendix for details of these submodels.

With the population model of component BHs defined above, then the overall population model for BBHs is expressed as

$$\pi(\lambda|\Lambda) \propto \pi(m_1, \chi_1, \cos\theta_1|\Lambda)\pi(m_2, \chi_2, \cos\theta_2|\Lambda)$$

$$\mathcal{F}_{\text{pair}}(m_1, m_2|\beta)P_z(z|\gamma), \tag{2}$$

where $\mathcal{F}_{\mathrm{pair}}(m_1,m_2|\beta)=(m_2/m_1)^{\beta}$ is the pairing function and $P_z(z|\gamma)$ is the redshift distribution, assuming a merger rate evolution $R(z)=R_0(1+z)^{\gamma}$.

Hierarchical Bayesian Inference. We perform hierarchical Bayesian inference to constrain our model parameters. The likelihood is constructed assuming an inhomogeneous Poisson process. For a series of measurements of $N_{\rm obs}$ events \vec{d} , and assuming a redshift evolving merger rate $R \propto (1+z)^{\gamma}$, the likelihood for the hyper-parameters Λ can be inferred via [35–37]

$$\mathcal{L}(\vec{d} \mid \mathbf{\Lambda}) \propto N^{N_{\text{obs}}} \exp(-N\eta(\mathbf{\Lambda})) \prod_{i}^{N_{\text{obs}}} \frac{1}{n_{i}} \sum_{k}^{n_{i}} \frac{\pi(\theta_{i}^{k} \mid \mathbf{\Lambda})}{\pi(\theta_{i}^{k} \mid \varnothing)},$$
(3)

where N is the expected number of mergers during the observation period and $\eta(\Lambda)$ is the detection efficiency. Following the procedures described in [38], we use the injection campaign from [39] (https://zenodo.org/records/16740128) to estimate $\eta(\Lambda)$. The n_i posterior samples for the ith event and the default prior $\pi(\theta^k \mid \varnothing)$ are taken from the data releases of [25, 40, 41] (https://gwosc.org/eventapi/html/GWTC/). We constrain the total Monte Carlo integration uncertainty as

 $\ln \delta_{\rm tot} < 1$ [38], ensuring an accurate likelihood evaluation. We adopt the same detection threshold as [38] (false alarm rate FAR < 1/yr), yielding 153 BBH events. Note that GW190814 is excluded from our analysis due to its unclear nature [42]. We use the BILBY package [43] with PYMULTINEST sampler [44] to obtain the Bayesian evidences and posteriors of the hyper-parameters for each model.

Results. In the top panel of Figure 1, we show the component-mass versus spin-magnitude distribution of each event in GWTC-4.0. Notably, the O4a data reveal a group of BHs with low spins but high masses (> $50M_{\odot}$) that was largely absent in GWTC-3 (this is also evident in Figure 2 of [19]). We therefore anticipate that the mass cutoff of the low-spin group (i.e., $m_{\rm max,1}$) will be higher than previously reported. Motivated by such a fact, we performed the Bayesian inference with the population model described above. The population-informed mass-spin distribution is presented in the bottom panel of Figure 1. Clearly, there is a distinct group of low-spin but massive black holes, which is the focus of this work.

Consistent with GWTC-3 studies [18, 19, 23], we identify two subpopulations of BHs in GWTC-4.0, which are well separated in the component-mass versus spin-magnitude parameter space (see Figure 2). The second subpopulation's spin magnitudes peak at ~ 0.8 , and its mass distribution extends beyond $100M_{\odot}$. These features are most naturally explained if these BHs are remnants of earlier mergers [5], especially for aligned BBH mergers in active galactic nucleus disks [34, 46]. Additionally, some events may contain double high-spin BHs, as was also suggested in [14, 47–49].

In the left panel of Figure 3, we plot the posterior distribution of the mass cutoff for the low-spin BH population and find $m_{\text{max},1} = 68.5^{+19.9}_{-18.3} M_{\odot}$ (90% credibility). This cutoff, although higher than the M_{low} predicted in many works [8-10, 50], is possible for a relatively low $^{12}C(\alpha,\gamma)^{16}O$ reaction rate [11, 12]. Combining the $M_{\rm BH}$ - σ relation from Figure 10 (where σ is the uncertainty in the $^{12}C(\alpha, \gamma)^{16}O$ reaction rate) of Mehta et al. [12] with the reaction rate from deBoer et al. [45], we infer $S_{300\text{keV}} = 108.6^{+54.9}_{-26.5} \text{ keV b } (90\% \text{ confidence interval};$ see Figure 3), somewhat lower than the commonly adopted $S_{300 \mathrm{keV}} = 140 \pm 21^{+18}_{-11} \mathrm{\ keV} \mathrm{\ b}$ recommended by deBoer et al. [45]. Note that with new measurements of the ground state asymptotic normalization coefficient, Shen et al. [50] obtained a higher value of $S_{300 \text{keV}} \approx 170 \text{ keV}$ b, which suggests a $M_{\rm low} \approx 52 M_{\odot}$, plausibly in tension with our $m_{\rm max,1}$. However, a recent Bayesian analysis favors a value of $S_{300 \text{keV}} \approx 130 \text{ keV b}$ [51]. We also remark that newly formed BHs could gain mass via (fallback) accretion, but such accretion would considerably increase the spin; the fact that these BHs have spins < 0.4 suggests any mass growth was < 20%. In light of these considerations, we conclude that the high mass cutoff of the low-spin BHs $(m_{\text{max},1})$ likely indeed corresponds to M_{low} , as expected in the PISN scenario.

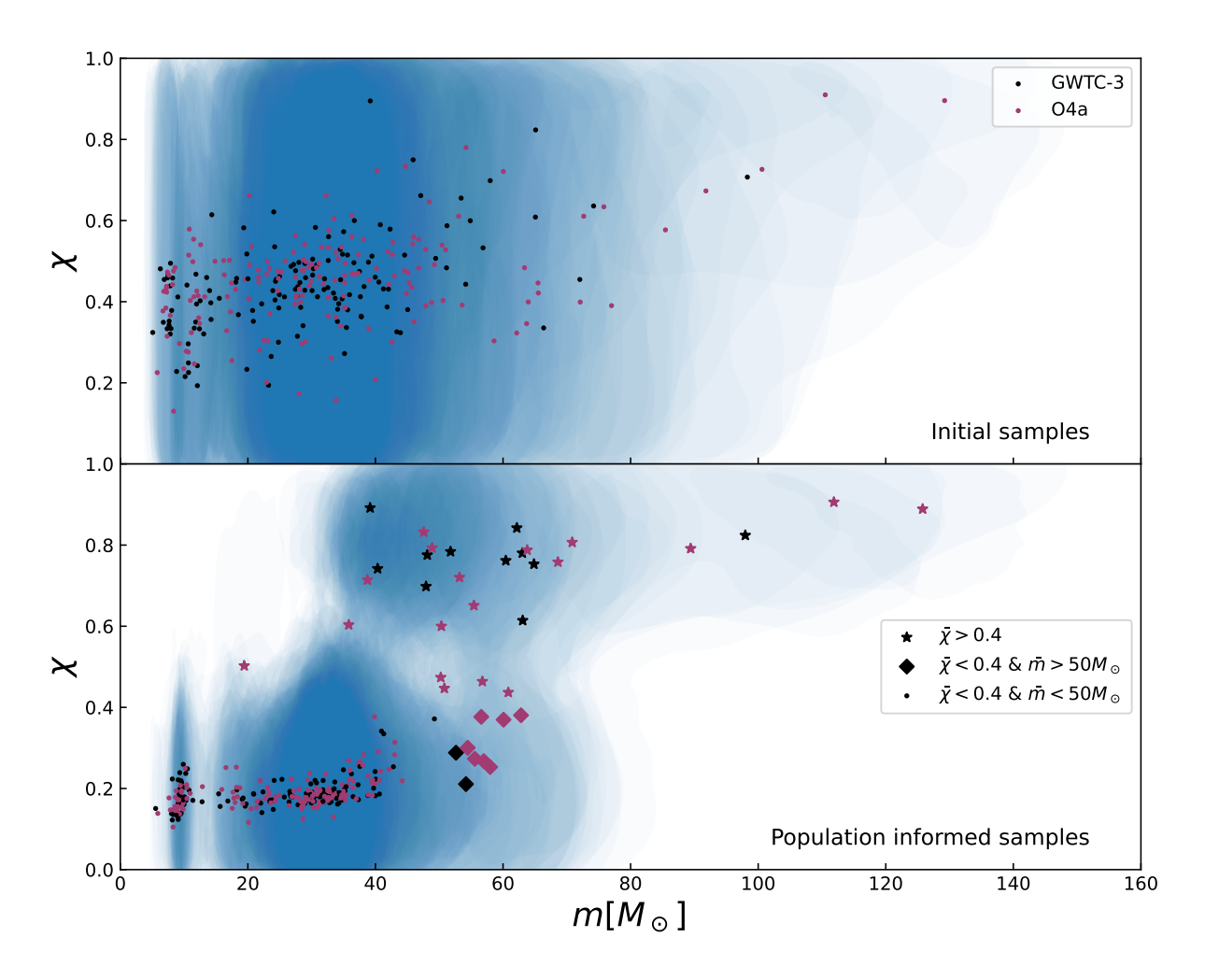


FIG. 1. Top panel: The mass-spin distribution of the black holes, the points (black for GWTC-3, while purple for O4a) are for the median values $(\bar{m},\bar{\chi})$, and the shaded regions are for the 90% credible intervals. An attractive feature we find is the emergence of a new group of $\gtrsim 50 M_{\odot}$ black holes likely with low spins in the O4a data. Bottom panel: component-mass and spin-magnitude distributions of events in GWTC-4, reweighed by a population-informed prior inferred in this work. The points, diamonds, and stars are for the low-spin low-mass ($\bar{\chi} < 0.4$, $\bar{m} < 50 M_{\odot}$), low-spin high-mass ($\bar{\chi} < 0.4$, $\bar{m} > 50 M_{\odot}$), and high-spin ($\bar{\chi} > 0.4$) BHs. Orange and black are for primary and secondary component, respectively.

Identifying a population of low-spin, high-mass BHs initially formed in massive single-star evolution would also establish the dynamical capture channel for BBH formation. With a larger sample anticipated in the upcoming O5 run, subtracting this component could yield a more precise estimate of $M_{\rm low}$ (which is $\approx m_{\rm max,1}$) and thus $S_{300{\rm keV}}$. Hendriks et al. [52] showed that shifting the expected carbon-oxygen core mass range upward by $\sim 10 M_{\odot}$ brings the predicted rate of hydrogen-poor superluminous supernovae into better agreement with observations. In such a scenario, they predicted no cutoff in the BH mass function up to $\sim 64 M_{\odot}$, which may have been confirmed by this work.

Discussion. With the enlarged GWTC-4.0 sample, we recover a low-spin yet high-mass BH group extending to $\gtrsim 60-70\,M_\odot$, whose properties are difficult to attribute to hierarchical growth [5, 53, 54]. One potential interpretation

for this low-spin, high-mass black hole group is the collapse of massive single stars [11]. It was realized by Winch et al. [32] that blue supergiant progenitors with small cores but large hydrogen envelopes at low metallicity could directly collapse to black holes as massive as $\sim 93 M_{\odot}$. Such massive first-generation BHs (with low spins) can be assembled via dynamical capture in dense environments [5]. In this scenario, the spins of these BHs would be isotropic, unless being oriented in gas-rich environments [55]. Unfortunately, the current sample of low-spin, high-mass BH events is too small to test this expectation, and analyzing the spin orientation distribution for low-spin events is inherently challenging [56]. If the mass of these objects were instead inherited from the CO core of massive stars, they raise the lower edge of the PIMG to $M_{\rm low}=68.5^{+19.9}_{-18.3}M_{\odot}$, and implies $S_{300{\rm keV}}=108.6^{+54.9}_{-26.5}\,{\rm keV}$ b.

It is the time to understand the difference of the cutoff

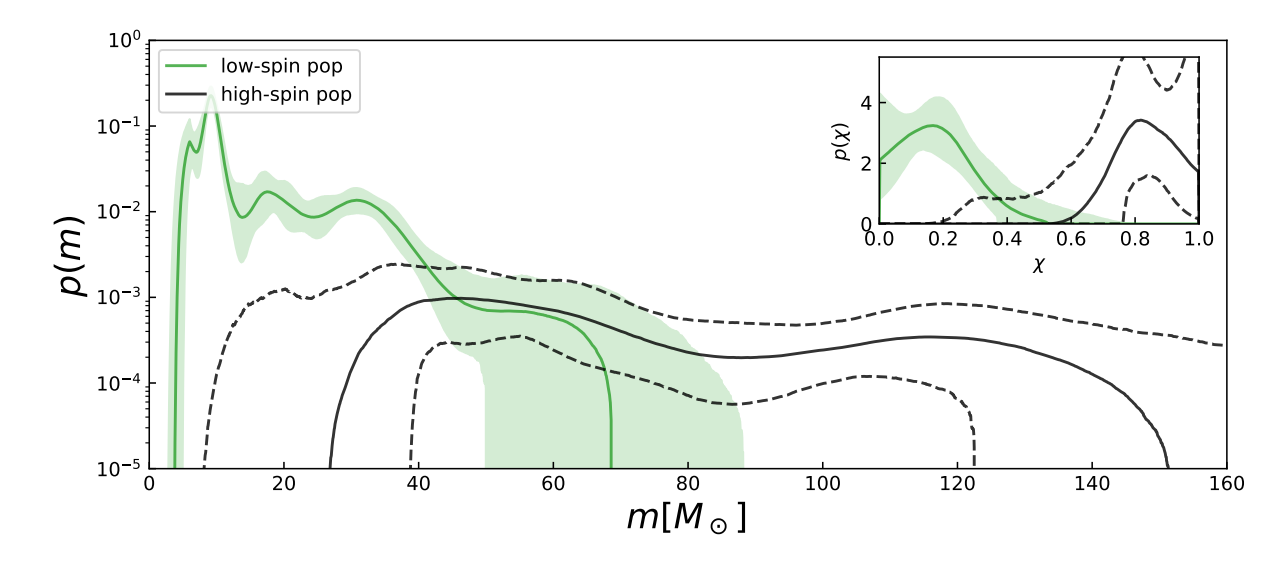


FIG. 2. The reconstructed component-mass and spin-magnitude distributions. The solid lines (dashed lines / shaded regions) indicate the median values and 90% credible regions for different subpopulations.

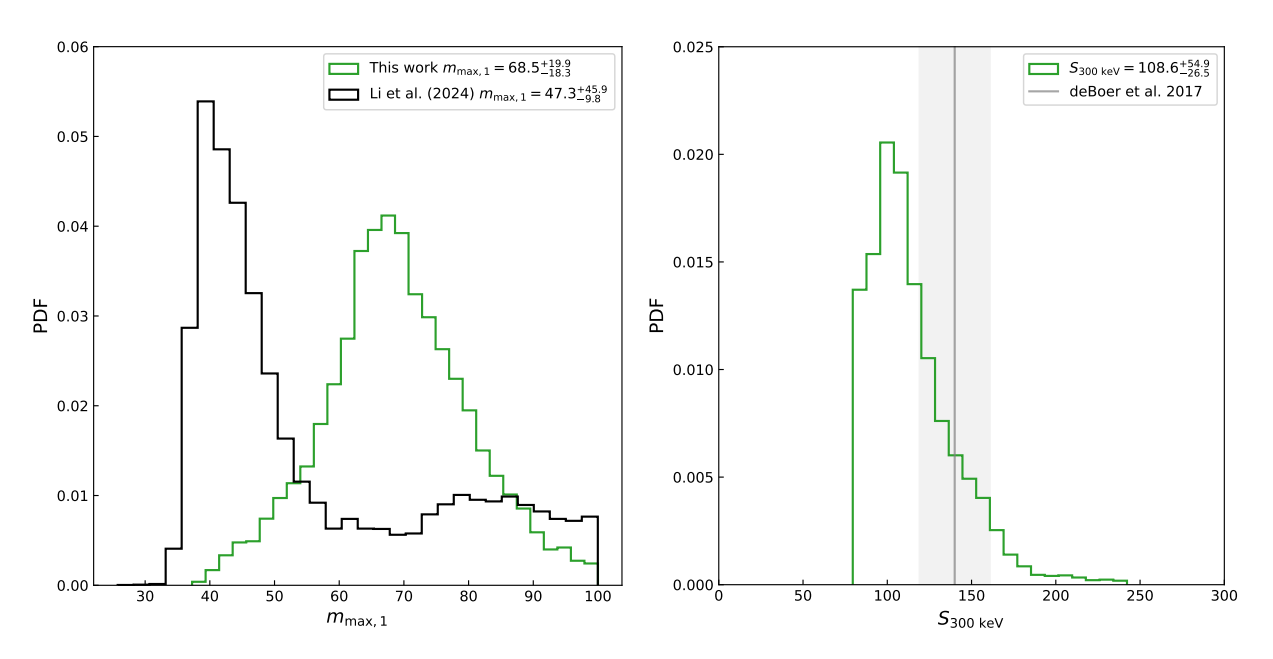


FIG. 3. The left panel is the probability distribution of the maximum mass $(m_{\text{max},1})$ of the low-spin group, and we have $m_{\text{max},1} = 68.5^{+19.8}_{-18.5} M_{\odot}$. In comparison to [19], the peak of the current probability distribution of the maximum mass is significantly higher. The right panel is the evaluated S factor of $^{12}C(\alpha,\gamma)^{16}O$ reaction at 300 keV assuming that $m_{\text{max},1}$ represents M_{low} . The value of $S_{300\text{keV}}$ recommended by [45] (1σ region including the model uncertainty) is also plotted for comparison.

masses reported for the first-generation population in some recent literature. Tong et al. [26] focused on the mass function of the secondary BHs (assumed to trace stellar-origin black holes) and, within that framework, they reported a cutoff at $\approx 45 M_{\odot}$. However, their assumption may break down if the secondary component is a mixture that includes higher-generation secondaries; for this possibility, see the square markers in Fig. 4 from our analysis. Very recently, with a flexible model, Ray & Kalogera [27] argued that the

 m_2 cutoff at $\sim 40-50 M_{\odot}$ reported in [26] may be caused by the strong prior assumptions, and the intrinsic value should be higher. In our analysis, there is no good candidate for low-spin secondary BHs above $\sim 50 M_{\odot}$ (note that some high-spin objects are heavier). But this is likely just a coincidence, since for a $m_{\rm max,1}\approx 68 M_{\odot}$ and a typical $q\sim 0.7$ (see Figure 4), the mass function of the secondary BHs will get suppressed at $\geq q m_{\rm max,1} \sim 45 M_{\odot}$. So, at least in our scenario, it is improper to interpret the lack of

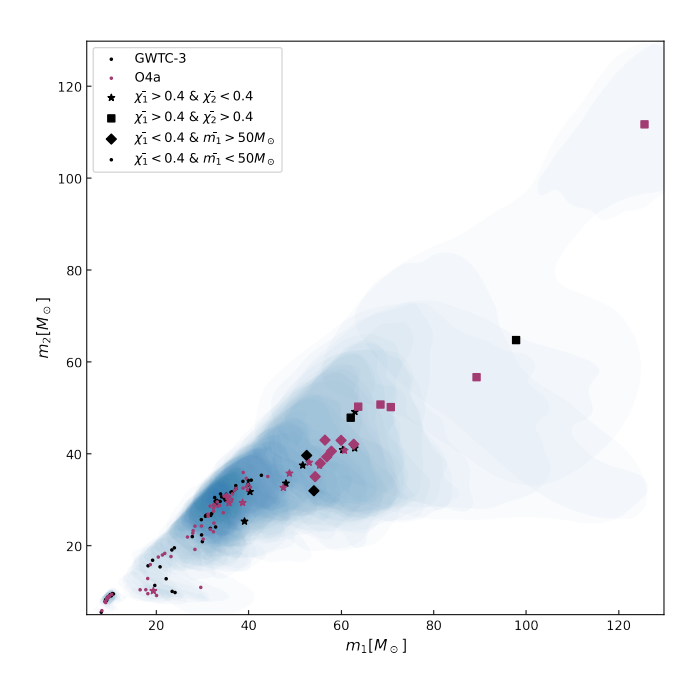


FIG. 4. Primary-mass versus secondary-mass distributions of events in GWTC-3 and O4a, reweighed by a population-informed prior inferred in this work. The points, diamonds, and stars / squares are for the low-spin low-mass ($\bar{\chi_1}<0.4,\,\bar{m_1}<50M_\odot$), low-spin high-mass ($\bar{\chi_1}<0.4,\,\bar{m_1}>50M_\odot$), and high-spin ($\bar{\chi_1}>0.4,\,\bar{\chi_2}<0.4$) / ($\bar{\chi_1}>0.4,\,\bar{\chi_2}>0.4$) BBHs.

low-spin m_2 at $\geq 45 M_{\odot}$ as the low edge of the PIMG. Antonini et al. [28] reported a rapid effective-spin transition at $45.3^{+6.5}_{-4.8} \rm{M}_{\odot}$ and interpreted it as $M_{\rm low}$, in agreement with the spin-magnitude-based analysis result by Wang et al. [18] in 2022 with the GWTC-3 data. We note that in Figure 2, the declining mass function of the low-spin population intersects the rising mass function of the high-spin population at $\approx 45 M_{\odot}$. This can explain why, in the analyses assuming a mass-dependent spin-magnitude or effective spin distribution to model a transition between the two subpopulations, the authors obtained a dividing mass of $\approx 45 M_{\odot}$ [18, 28]. However, this mass is not necessary to mark the onset of PIMG and a higher value is plausible.

The ongoing O4 observing run of the LIGO/Virgo/KAGRA (LVK) collaboration is rapidly expanding the catalog of detected binary black hole (BBH) events. The BBH sample is expected to be doubled, when all events of the O4 run have been released. At that time the properties of the first-generation BHs as well as the stellar evolution theories will be further revealed/probed. The prospect is even more promising since LIGO/Virgo/KAGRA will be further upgraded.

Acknowledgments. This work is supported by the National Natural Science Foundation of China (No. 12233011, No. 12203101, No. 12303056, No. 12503059, No. 123B2045), the General Fund (No. 2024M753495) of the China Postdoctoral Science Foundation, and the Pri-

ority Research Program of the Chinese Academy of Sciences (No. XDB0550400). This research has made use of data and software obtained from the Gravitational Wave Open Science Center (https://www.gw-openscience.org), a service of LIGO Laboratory, the LIGO Scientific Collaboration and the Virgo Collaboration. LIGO is funded by the U.S. National Science Foundation. Virgo is funded by the French Centre National de Recherche Scientifique (CNRS), the Italian Istituto Nazionale della Fisica Nucleare (INFN) and the Dutch Nikhef, with contributions by Polish and Hungarian institutes.

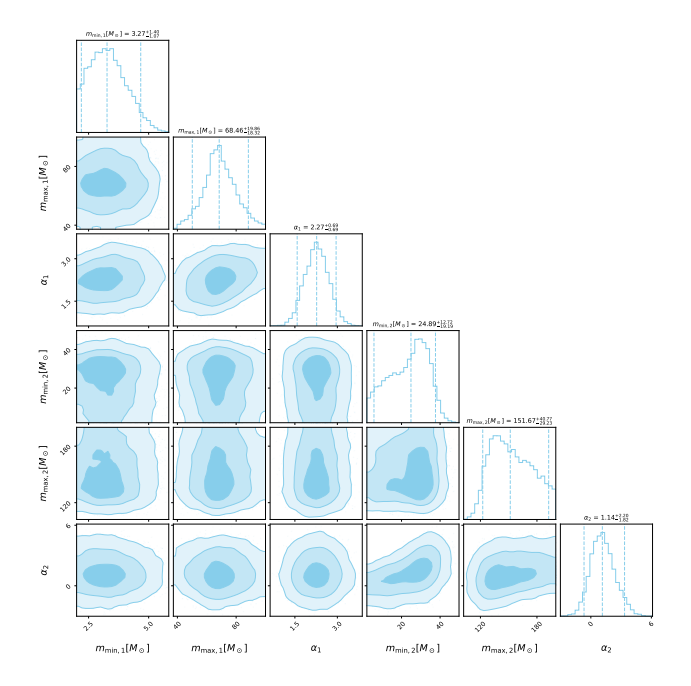


FIG. 5. Parameters of mass functions for the two subpopulations. The values are for median and 90% credible intervals.

Sub-models

In order to obtain data-driven results, the mass and spin distributions of each subpopulation are modeled with flexible formula. The mass functions are expressed as [33, 57],

$$P_{m,i}(m|\Lambda) \propto m^{-\alpha_i} e^{f(m|\{f_j^i\}_{j=1}^n)} B(m),$$
 (4)

where B(m) is the function characterizing the boundary of the mass distribution defined as

$$B(m) = \begin{cases} 0 & \text{if } m > m_{\text{max,i}} \\ \mathcal{S}(m|m_{\text{min,i}}, \delta_{\text{m,i}}) & \text{if } m_{\text{min,i}} < m < m_{\text{max,i}} \\ 0 & \text{if } m < m_{\text{min,i}} \end{cases}$$

 $\mathcal{S}(m|m_{\min,i},\delta_{\mathrm{m,i}})$ is the smooth function defined in [36]. For the first / second subpopulation, we set 15 / 10 knots $(\{f_j^1\}_{j=1}^{15})$ / $(\{f_j^2\}_{j=1}^{10})$) linearly in the log space between $[6-100]M_{\odot}$ / $[10-150]M_{\odot}$. This is because the first (second) subpopulation dominates the lower (higher) mass range.

The spin magnitudes and cosine-tilt-angles are also described with flexible models [33, 58],

$$P_{\chi,i}(\chi|\Lambda) \propto e^{x(\chi|\{x_j^i\}_{j=1}^n)} [\chi_{\min,i}, \chi_{\max,i}], \qquad (6)$$

$$P_{\cos\theta,i}(\cos\theta|\Lambda) \propto e^{t(\cos\theta|\{t_j^i\}_{j=1}^n)}[-1,1], \qquad (7)$$

we set 5 and 4 knots $(\{x_j^i\}_{j=1}^5, \{t_j^i\}_{j=1}^4)$ to interpolate the perturbation function of spin magnitude and cosine-tiltangle distributions in each subpopulation. All the parameters are summarized in Table I, and the posterior distribution of the parameters for mass functions are displayed in Figure 5.

- * Contributed equally.
- Corresponding author: yzfan@pmo.ac.cn
- [1] B. P. Abbott *et al.*, Observation of Gravitational Waves from a Binary Black Hole Merger, Phys Rev Lett **116**, 061102 (2016), arXiv:1602.03837.
- [2] The LIGO Scientific Collaboration *et al.*, Tests of General Relativity with GWTC-3, arXiv e-prints, arXiv:2112.06861 (2021), arXiv:2112.06861.
- [3] A. G. Abac *et al.*, GW250114: Testing Hawking's Area Law and the Kerr Nature of Black Holes, Phys Rev Lett **135**, 111403 (2025), arXiv:2509.08054.
- [4] S.-P. Tang, H.-T. Wang, Y.-J. Li, and Y.-Z. Fan, Verification of the Black Hole Area Law with GW230814, arXiv e-prints , arXiv:2509.03480 (2025), arXiv:2509.03480.
- [5] D. Gerosa and M. Fishbach, Hierarchical mergers of stellarmass black holes and their gravitational-wave signatures, Nature Astronomy 5, 749 (2021), arXiv:2105.03439.
- [6] I. Mandel and A. Farmer, Merging stellar-mass binary black holes, Phys Rep 955, 1 (2022), arXiv:1806.05820.
- [7] Z. Barkat, G. Rakavy, and N. Sack, Dynamics of Supernova Explosion Resulting from Pair Formation, Phys Rev Lett 18, 379 (1967).
- [8] K. Belczynski et al., The effect of pair-instability mass loss on black-hole mergers, A&A 594, A97 (2016), arXiv:1607.03116.
- [9] M. Spera and M. Mapelli, Very massive stars, pair-instability supernovae and intermediate-mass black holes with the sevn code, MNRAS 470, 4739 (2017), arXiv:1706.06109.
- [10] S. E. Woosley, Pulsational Pair-instability Supernovae, ApJ 836, 244 (2017), arXiv:1608.08939.
- [11] S. E. Woosley and A. Heger, The Pair-instability Mass Gap for Black Holes, ApJL912, L31 (2021), arXiv:2103.07933.
- [12] A. K. Mehta *et al.*, Observing Intermediate-mass Black Holes and the Upper Stellar-mass gap with LIGO and Virgo, ApJ **924**, 39 (2022), arXiv:2105.06366.
- [13] B. P. Abbott *et al.*, GWTC-1: A Gravitational-Wave Transient Catalog of Compact Binary Mergers Observed by LIGO and Virgo during the First and Second Observing Runs, Physical Review X **9**, 031040 (2019), arXiv:1811.12907.
- [14] R. Abbott *et al.*, GW190521: A Binary Black Hole Merger with a Total Mass of 150 M_{\odot} , Phys Rev Lett **125**, 101102 (2020), arXiv:2009.01075.
- [15] C. Kimball *et al.*, Evidence for Hierarchical Black Hole Mergers in the Second LIGO-Virgo Gravitational Wave Catalog, ApJL**915**, L35 (2021), arXiv:2011.05332.
- [16] Y.-Z. Wang et al., Black Hole Mass Function of Coalescing Binary Black Hole Systems: Is there a Pulsational Pair-instability Mass Cutoff?, ApJ 913, 42 (2021), arXiv:2104.02566.
- [17] E. J. Baxter, D. Croon, S. D. McDermott, and J. Sakstein, Find the Gap: Black Hole Population Analysis with an Astrophysically Motivated Mass Function, ApJL**916**, L16 (2021), arXiv:2104.02685.
- [18] Y.-Z. Wang et al., Potential Subpopulations and Assembling Tendency of the Merging Black Holes, ApJL941, L39 (2022), arXiv:2208.11871.

TABLE I. Summary of model parameters.

Parameter	Description	Prior
mass function		
$m_{ m min,i}[M_{\odot}]$	The minimum mass	U(2,50)
$m_{ m max,2}[M_{\odot}]$ / $m_{ m max,1}[M_{\odot}]$	The maximum mass	U(20,100) / U(20,200)
$lpha_i$	Slope index of the power-law mass function	U(-8,8)
$\delta_{ m m,i}[M_{\odot}]$	Smooth scale of the mass lower edge	U(0, 10)
$\{f_j^1\}_{j=2}^{14} / \{f_j^2\}_{j=2}^9$	Interpolation values of perturbation function	$\mathcal{N}(0,1)$
r_2	mixture fraction for the second subpopulation	U(0,1)
constraints		$m_{\rm min,i} < m_{\rm max,i}$
eta_q	Slope index of the mass-ratio distribution	U(-8,8)
Spin distribution		
$\chi_{\mathrm{min},1}$ / $\chi_{\mathrm{min},2}$	Lower edge for χ distribution	0 / $U(0,0.8)$
$\chi_{\rm max,1}$ / $\chi_{\rm max,2}$	Upper edge for χ distribution	U(0.2,1) / 1
$\{x_j^i\}_{j=1}^5$	Interpolation values for χ distribution	$\mathcal{N}(0,1)$
$\{t_j^i\}_{j=1}^4$	Interpolation values for $\cos \theta$ distribution	$\mathcal{N}(0,1)$
Rate evolution model		
$\lg(R_0[\mathrm{Gpc}^{-3}\ \mathrm{yr}^{-1}])$	Local merger rate density	U(-3,3)
γ	Slope of the power-law	U(-8,8)

Note: $U, \mathcal{N}, \mathcal{G}$ are for Uniform, Normal distribution, and Gaussian distribution.

- [19] Y.-J. Li, Y.-Z. Wang, S.-P. Tang, and Y.-Z. Fan, Resolving the Stellar-Collapse and Hierarchical-Merger Origins of the Coalescing Black Holes, Phys Rev Lett 133, 051401 (2024), arXiv:2303.02973.
- [20] Y.-J. Li, S.-P. Tang, S.-J. Gao, D.-C. Wu, and Y.-Z. Wang, Exploring Field-evolution and Dynamical-capture Coalescing Binary Black Holes in GWTC-3, ApJ 977, 67 (2024), arXiv:2404.09668.
- [21] G. Pierra, S. Mastrogiovanni, and S. Perriès, The spin magnitude of stellar-mass binary black holes evolves with the mass: evidence from gravitational wave data, arXiv e-prints, arXiv:2406.01679 (2024), arXiv:2406.01679.
- [22] W.-H. Guo *et al.*, The Heavier the Faster: A Subpopulation of Heavy, Rapidly Spinning and Quickly Evolving Binary Black Holes, ApJ 975, 54 (2024), arXiv:2406.03257.
- [23] F. Antonini, I. M. Romero-Shaw, and T. Callister, Star Cluster Population of High Mass Black Hole Mergers in Gravitational Wave Data, Phys Rev Lett 134, 011401 (2025), arXiv:2406.19044.
- [24] Y.-J. Li, Y.-Z. Wang, S.-P. Tang, T. Chen, and Y.-Z. Fan, Revealing the χ_{eff} -q Correlation among Coalescing Binary Black Holes and Tentative Evidence for AGN-driven Hierarchical Mergers, ApJ **987**, 65 (2025), arXiv:2501.09495.
- [25] The LIGO Scientific Collaboration et al., GWTC-4.0: Updating the Gravitational-Wave Transient Catalog with Observations from the First Part of the Fourth LIGO-Virgo-KAGRA Observing Run, arXiv e-prints, arXiv:2508.18082 (2025), arXiv:2508.18082.
- [26] H. Tong *et al.*, Evidence of the pair instability gap in the distribution of black hole masses, arXiv e-prints, arXiv:2509.04151 (2025), arXiv:2509.04151.
- [27] A. Ray and V. Kalogera, Reexamining Evidence of a Pair-Instability Mass Gap in the Binary Black Hole

- Population, arXiv e-prints, arXiv:2510.18867 (2025), arXiv:2510.18867.
- [28] F. Antonini et al., Gravitational waves reveal the pair-instability mass gap and constrain nuclear burning in massive stars, arXiv e-prints, arXiv:2509.04637 (2025), arXiv:2509.04637.
- [29] S. Banagiri, E. Thrane, and P. D. Lasky, Evidence for Three Subpopulations of Merging Binary Black Holes at Different Primary Masses, arXiv e-prints, arXiv:2509.15646 (2025), arXiv:2509.15646.
- [30] N. Guttman, E. Payne, P. D. Lasky, and E. Thrane, Trends in the Population of Binary Black Holes Following the Fourth Gravitational-Wave Transient Catalog: a Data-Driven Analysis, arXiv e-prints, arXiv:2509.09876 (2025), arXiv:2509.09876.
- [31] S. Afroz and S. Mukherjee, Binary Black Hole Phase Space Discovers the Signature of Pair Instability Supernovae Mass Gap, arXiv e-prints, arXiv:2509.09123 (2025), arXiv:2509.09123.
- [32] E. R. J. Winch, J. S. Vink, E. R. Higgins, and G. N. Sabhahitf, Predicting the heaviest black holes below the pair instability gap, MNRAS 529, 2980 (2024), arXiv:2401.17327.
- [33] B. Edelman, B. Farr, and Z. Doctor, Cover Your Basis: Comprehensive Data-driven Characterization of the Binary Black Hole Population, ApJ 946, 16 (2023), arXiv:2210.12834.
- [34] Y.-J. Li, Y.-Z. Wang, S.-P. Tang, and Y.-Z. Fan, Aligned Hierarchical Black Hole Mergers in AGN disks revealed by GWTC-4, arXiv e-prints, arXiv:2509.23897 (2025), arXiv:2509.23897.
- [35] I. Mandel, W. M. Farr, and J. R. Gair, Extracting distribution parameters from multiple uncertain observations with selec-

- tion biases, MNRAS 486, 1086 (2019), arXiv:1809.02063.
- [36] R. Abbott *et al.*, Population Properties of Compact Objects from the Second LIGO-Virgo Gravitational-Wave Transient Catalog, ApJL**913**, L7 (2021), arXiv:2010.14533.
- [37] R. Abbott *et al.*, Population of Merging Compact Binaries Inferred Using Gravitational Waves through GWTC-3, Physical Review X 13, 011048 (2023), arXiv:2111.03634.
- [38] The LIGO Scientific Collaboration, the Virgo Collaboration, and the KAGRA Collaboration, GWTC-4.0: Population Properties of Merging Compact Binaries, arXiv e-prints, arXiv:2508.18083 (2025), arXiv:2508.18083.
- [39] R. Essick et al., Compact Binary Coalescence Sensitivity Estimates with Injection Campaigns during the LIGO-Virgo-KAGRA Collaborations' Fourth Observing Run, arXiv e-prints, arXiv:2508.10638 (2025), arXiv:2508.10638.
- [40] R. Abbott *et al.*, GWTC-2.1: Deep extended catalog of compact binary coalescences observed by LIGO and Virgo during the first half of the third observing run, Phys Rev D **109**, 022001 (2024), arXiv:2108.01045.
- [41] R. Abbott et al., GWTC-3: Compact Binary Coalescences Observed by LIGO and Virgo during the Second Part of the Third Observing Run, Physical Review X 13, 041039 (2023), arXiv:2111.03606.
- [42] R. Abbott *et al.*, GW190814: Gravitational Waves from the Coalescence of a 23 Solar Mass Black Hole with a 2.6 Solar Mass Compact Object, ApJL896, L44 (2020), arXiv:2006.12611.
- [43] G. Ashton *et al.*, BILBY: A User-friendly Bayesian Inference Library for Gravitational-wave Astronomy, ApJS 241, 27 (2019), arXiv:1811.02042.
- [44] J. Buchner, PyMultiNest: Python interface for MultiNest, Astrophysics Source Code Library, record ascl:1606.005, 2016, ascl:1606.005.
- [45] R. J. deBoer *et al.*, The 12 C(α , γ) 16 O reaction and its implications for stellar helium burning, Reviews of Modern Physics **89**, 035007 (2017), arXiv:1709.03144.
- [46] M. P. Vaccaro *et al.*, Impact of gas hardening on the population properties of hierarchical black hole mergers in active galactic nucleus disks, A&A **685**, A51 (2024), arXiv:2311.18548.
- [47] Y.-J. Li, S.-P. Tang, L.-Q. Xue, and Y.-Z. Fan, GW231123:

- a product of successive mergers from ~ 10 stellar-mass black holes, arXiv e-prints , arXiv:2507.17551 (2025), arXiv:2507.17551.
- [48] C. Adamcewicz, N. Guttman, P. D. Lasky, and E. Thrane, Do both black holes spin in merging binaries? Evidence from GWTC-4 and astrophysical implications, arXiv eprints, arXiv:2509.04706 (2025), arXiv:2509.04706.
- [49] G.-P. Li and X.-L. Fan, The Hierarchical Merger Scenario for GW231123, arXiv e-prints, arXiv:2509.08298 (2025), arXiv:2509.08298.
- [50] Y. Shen *et al.*, New Determination of the $^{12}\text{C}(\alpha, \gamma)^{16}\text{O}$ Reaction Rate and Its Impact on the Black-hole Mass Gap, ApJ **945**, 41 (2023).
- [51] A. M. Mukhamedzhanov, Bayesian Framework for the E1 and E2 Astrophysical Factors at 300 keV from Subthreshold and Ground-State Asymptotic Normalization Coefficients, arXiv e-prints, arXiv:2509.17102 (2025), arXiv:2509.17102.
- [52] D. D. Hendriks, L. A. C. van Son, M. Renzo, R. G. Izzard, and R. Farmer, Pulsational pair-instability supernovae in gravitational-wave and electromagnetic transients, MN-RAS 526, 4130 (2023), arXiv:2309.09339.
- [53] D. Gerosa and E. Berti, Are merging black holes born from stellar collapse or previous mergers?, Phys Rev D 95, 124046 (2017), arXiv:1703.06223.
- [54] M. Fishbach, D. E. Holz, and B. Farr, Are LIGO's Black Holes Made from Smaller Black Holes?, ApJL840, L24 (2017), arXiv:1703.06869.
- [55] B. McKernan and K. E. S. Ford, Constraining the LVK AGN channel with black hole spins, MNRAS 531, 3479 (2024), arXiv:2309.15213.
- [56] S. Vitale, M. Mould, and S. (Society Of Physicists Interested in Non-Aligned Spins, Long road to alignment: Measuring black hole spin orientation with expanding gravitational-wave datasets, Phys Rev D 112, 083015 (2025), arXiv:2505.14875.
- [57] B. Edelman, Z. Doctor, J. Godfrey, and B. Farr, Ain't No Mountain High Enough: Semiparametric Modeling of LIGO-Virgo's Binary Black Hole Mass Distribution, ApJ 924, 101 (2022), arXiv:2109.06137.
- [58] J. Golomb and C. Talbot, Searching for structure in the binary black hole spin distribution, Phys Rev D 108, 103009 (2023), arXiv:2210.12287.